

## **General Disclaimer**

### **One or more of the Following Statements may affect this Document**

- This document has been reproduced from the best copy furnished by the organizational source. It is being released in the interest of making available as much information as possible.
- This document may contain data, which exceeds the sheet parameters. It was furnished in this condition by the organizational source and is the best copy available.
- This document may contain tone-on-tone or color graphs, charts and/or pictures, which have been reproduced in black and white.
- This document is paginated as submitted by the original source.
- Portions of this document are not fully legible due to the historical nature of some of the material. However, it is the best reproduction available from the original submission.

# NASA TECHNICAL MEMORANDUM

NASA TM X-64944

(NASA-TM-X-64944) MOESSBAUER STUDIES IN  
ZINC-MANGANESE FERRITES FOR USE IN MEASURING  
SMALL VELOCITIES AND ACCELERATIONS WITH  
GREAT PRECISION (NASA) 35 p HC \$3.75

N75-26889

Unclas  
28027

CSCL 20L G3/76

## MÖSSBAUER STUDIES IN ZINC-MANGANESE FERRITES FOR USE IN MEASURING SMALL VELOCITIES AND ACCELERATIONS WITH GREAT PRECISION

By W. T. Escue, R. G. Gupta, and  
R. G. Mendiratta  
Electronics and Control Laboratory

June 13, 1975

**NASA**



*George C. Marshall Space Flight Center  
Marshall Space Flight Center, Alabama*

TECHNICAL REPORT STANDARD TITLE PAGE

1. REPORT NO. NASA TM X-64944		2. GOVERNMENT ACCESSION NO.		3. RECIPIENT'S CATALOG NO.	
4. TITLE AND SUBTITLE Mössbauer Studies in Zinc-Manganese Ferrites for use in Measuring Small Velocities and Accelerations with Great Precision				5. REPORT DATE June 13, 1975	
				6. PERFORMING ORGANIZATION CODE	
7. AUTHOR(S) W.T. Escue, R.G. Gupta,* and R.G. Mendiratta*				8. PERFORMING ORGANIZATION REPORT #	
9. PERFORMING ORGANIZATION NAME AND ADDRESS George C. Marshall Space Flight Center Marshall Space Flight Center, Alabama 35812				10. WORK UNIT NO.	
				11. CONTRACT OR GRANT NO.	
12. SPONSORING AGENCY NAME AND ADDRESS National Aeronautics and Space Administration Washington, D.C. 20546				13. TYPE OF REPORT & PERIOD COVERED Technical Memorandum	
				14. SPONSORING AGENCY CODE	
15. SUPPLEMENTARY NOTES Prepared by Electronics and Control Laboratory, Science and Engineering *Physics Department, Indian Institute of Technology, New Delhi - 110029, India.					
16. ABSTRACT <p>The Mössbauer effect has been very effectively used to study the nuclear hyperfine interactions. This has become possible because the line widths obtained in Mössbauer experimentation are small as compared to the characteristic energies of the interaction of nuclei with their surroundings. The primary objective of the work reported herein was to use Mössbauer spectroscopy for a systematic study of the magnetic behavior of manganese and zinc in mixed ferrites.</p>					
17. KEY WORDS			18. DISTRIBUTION STATEMENT Unclassified - Unlimited  <i>W. T. Escue</i>		
19. SECURITY CLASSIF. (of this report) Unclassified		20. SECURITY CLASSIF. (of this page) Unclassified		21. NO. OF PAGES 35	22. PRICE NTIS

## TABLE OF CONTENTS

	Page
INTRODUCTION . . . . .	1
GENERAL STRUCTURE OF FERRITES . . . . .	2
SAMPLE PREPARATION . . . . .	4
EXPERIMENTAL PROCEDURE . . . . .	5
RESULTS AND DISCUSSION . . . . .	7
SUMMARY AND CONCLUSIONS . . . . .	25
REFERENCES . . . . .	27

PRECEDING PAGE BLANK NOT FILMED

## LIST OF ILLUSTRATIONS

Figure	Title	Page
1.	Tetrahedrally and octahedrally coordinated metal ions . . . . .	3
2.	Block diagram of Mössbauer spectrometer . . . . .	6
3.	Mössbauer spectrum of $\text{MnFe}_2\text{O}_4$ . . . . .	8
4.	Mössbauer spectrum of $\text{Zn}_{0.1}\text{Mn}_{0.9}\text{Fe}_2\text{O}_4$ . . . . .	9
5.	Mössbauer spectrum of $\text{Zn}_{0.2}\text{Mn}_{0.8}\text{Fe}_2\text{O}_4$ . . . . .	10
6.	Mössbauer spectrum of $\text{Zn}_{0.3}\text{Mn}_{0.7}\text{Fe}_2\text{O}_4$ . . . . .	11
7.	Mössbauer spectrum of $\text{Zn}_{0.4}\text{Mn}_{0.6}\text{Fe}_2\text{O}_4$ . . . . .	12
8.	Mössbauer spectrum of $\text{Zn}_{0.5}\text{Mn}_{0.5}\text{Fe}_2\text{O}_4$ . . . . .	13
9.	Mössbauer spectrum of $\text{Zn}_{0.6}\text{Mn}_{0.4}\text{Fe}_2\text{O}_4$ . . . . .	14
10.	Mössbauer spectrum of $\text{Zn}_{0.7}\text{Mn}_{0.3}\text{Fe}_2\text{O}_4$ . . . . .	15
11.	Mössbauer spectrum of $\text{Zn}_{0.8}\text{Mn}_{0.2}\text{Fe}_2\text{O}_4$ . . . . .	16
12.	Mössbauer spectrum of $\text{Zn}_{0.9}\text{Mn}_{0.1}\text{Fe}_2\text{O}_4$ . . . . .	17
13.	Mössbauer spectrum of $\text{ZnFe}_2\text{O}_4$ . . . . .	18

## LIST OF TABLES

Table	Title	Page
1.	Isomer Shift and Magnetic Hyperfine Field for Samples Having Low Concentration of Zinc . . . . .	19
2.	Values of Spin Correlation Time $T_s$ and Spin Flip-Flop Frequency $\omega_s$ for a Few Samples . . . . .	22
3.	Isomer Shift and Quadrupole Splitting in Mixed Mn-Zn Ferrite with a High Concentration of Zinc . . . . .	25

# MÖSSBAUER STUDIES IN ZINC-MANGANESE FERRITES FOR USE IN MEASURING SMALL VELOCITIES AND ACCELERATIONS WITH GREAT PRECISION

## INTRODUCTION

Of all the fundamental discoveries that have been made in recent years, the discovery of the Mössbauer effect which brought the 1961 Nobel Prize in Physics to Rudolf Ludwig Mössbauer [1-3], a German physicist, has proved itself as the most powerful probe in investigating the nuclear and solid state properties of matter. This effect has provided an increasingly important interdisciplinary research tool to be used not only by nuclear and solid state physicists but also by physical and inorganic chemists, biologists, geologists, and many others in the solution of a wide range of scientific problems.

The Mössbauer effect has been very effectively used to study the nuclear hyperfine interactions. This has become possible because the line widths obtained in Mössbauer experimentation are small as compared to the characteristic energies of the interaction of nuclei with their surroundings. The primary objective of the work reported herein was to use Mössbauer spectroscopy for a systematic study of the magnetic behavior of manganese and zinc in mixed ferrites.

Ferrites, which are a broad class of complex magnetic oxides containing  $\text{Fe}^{3+}$  and other metal ions, are materials of technological importance. They have been found to be of immense industrial use, and their devices have found enormous applications in space research as well as in telecommunication programs. Interest in the, so called, mixed ferrites is primarily due to a substantial reduction in the Curie temperature, an increase in the room temperature permeability, and a decrease in the coercive force.

Intensive studies [4,5] of many properties of mixed zinc ferrite systems have been made. Of all these ferrites, Mn-Zn ferrites are of great practical importance because they have high saturation magnetization, low losses, and a relatively high Curie temperature. Also, the magnetostriction and crystal anisotropy of these ferrites are very weak. A considerable number of reports [6-13] have been published on Ni-Zn, Li-Zn, Co-Zn, Mg-Zn ferrites by different Mössbauer groups. No consistent agreement, however, exists between the various works reported; in fact, large discrepancies are observed in the literature.

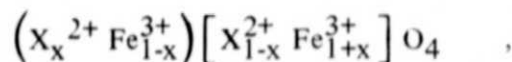
A limited number of reports have been published on Mn-Zn ferrite systems using Mössbauer spectroscopy. Cser et al. [14] has concluded that four sets of sextets exist in the observed Mössbauer spectra. They attribute the various six-line patterns to  $\text{Fe}^{3+}$  ions at the B-site in different environments; that is, different numbers of Zn ions in the immediate neighborhood of  $\text{Fe}^{3+}$ . Köing [15] has studied the  $\text{Mn}_{0.6}\text{Zn}_{0.4}\text{Fe}_2\text{O}_4$  system using the Mössbauer technique and has compared his results with those obtained using neutron diffraction methods. No definite conclusions, however, were drawn.

As already stated, mixed ferrites of manganese and zinc with various compositions were made by the authors in an effort to better understand those systems for which various theories have been proposed.

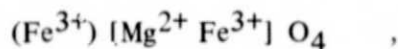
### GENERAL STRUCTURE OF FERRITES

Ferrites, which are essentially solid crystalline solutions of iron and other metals, are found to be chemically inert. X-ray studies have revealed [16-18] that ferrites have a spinel structure having composition  $XY_2O_4$ , where X represents a divalent ion such as  $Mg^{2+}$ ,  $Zn^{2+}$ ,  $Mn^{2+}$ ,  $Cd^{2+}$ , and Y represents a trivalent ion such as  $Fe^{3+}$ ,  $Al^{3+}$ . The structure is essentially cubic with 8 molecules per unit cell having 32 anions and 24 cations. It can be characterized as a face-centered cubic lattice having an array of oxygen ions with metal atoms located in the interstices of oxygen ions. These interstitial sites, 96 of which are in a unit cell, are of two types: sites (called the A-sites) where the metal ions are tetrahedrally coordinated with 4 oxygen neighbors, and sites (called the B-sites) where the metal ions are octahedrally coordinated with 6 neighboring oxygen ions. These two types of sites are shown in Figure 1. It is easy to see that in a unit cell there are 64 A-sites and 32 B-sites. However, of these 64 tetrahedral A-sites and 32 octahedral B-sites, only 8 and 16, respectively, are occupied by the metal ions.

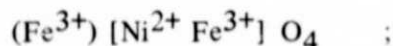
Ferrites can be classified in two extreme categories: inverse and normal ferrites. In the inverse ferrites, the A-sites are occupied by trivalent metal ions only and the B-sites are occupied by an equal number of trivalent and divalent metal ions. In normal ferrites, however, the A-sites are occupied by divalent metal ions and the B-sites are occupied by trivalent metal ions. In general, the distribution of ions in ferrites can be written as



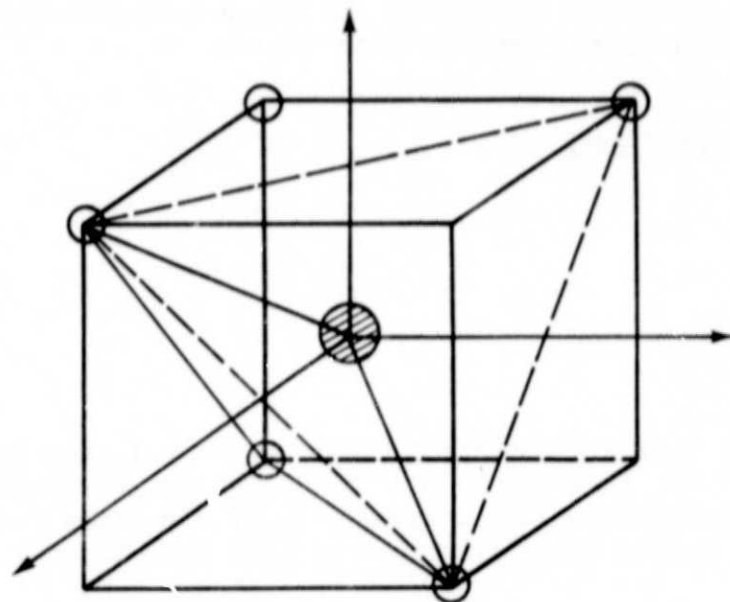
where the curved and square brackets contain A- and B-sites, respectively. Néel proposed the formation of two sublattices in such compounds: A-sublattice (curved bracket) and B-sublattice (square brackets). It is clear that  $x = 0$  corresponds to the case of an inverse ferrite, examples of which are magnesium and nickel ferrites with their respective formulas





and

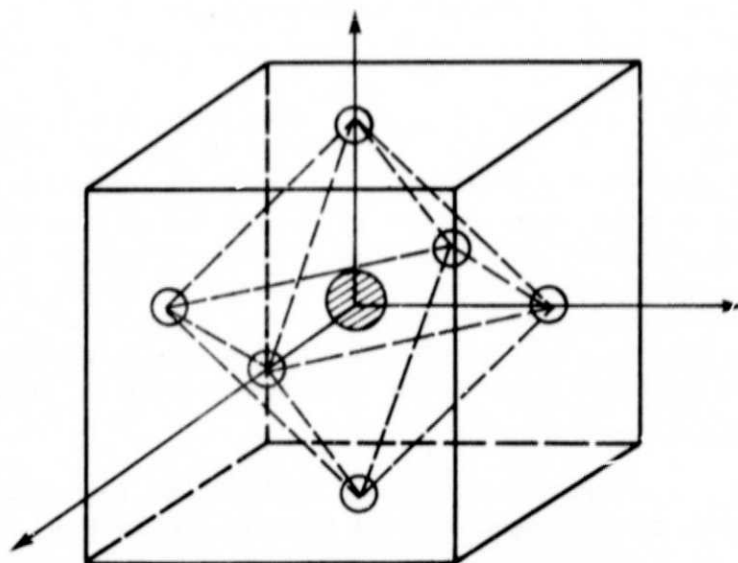






TETRAHEDRAL COORDINATION

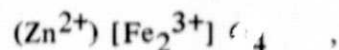
-  METAL ION
-  OXYGEN ION



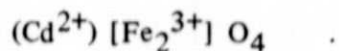
OCTAHEDRAL COORDINATION

Figure 1. Tetrahedrally and octahedrally coordinated metal ions.

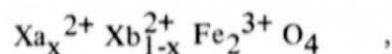
whereas  $x = 1$  corresponds to a normal ferrite, common examples of which are zinc and cadmium ferrites given respectively by the formulas



and



Intermediate values of  $x$  correspond to ferrites that are neither pure inverse ferrites or pure normal ferrites. The degree of inversion decreases with an increasing value of  $x$ . In the spinel structure if a ferrite has two or more different divalent ions, it is called a mixed ferrite. A mixed ferrite of divalent ions can be represented by

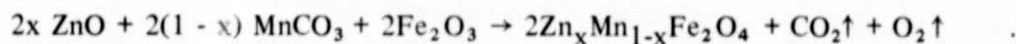


where  $\text{Xa}^{2+}$  and  $\text{Xb}^{2+}$  are two different metal divalent ions.

### SAMPLE PREPARATION

The properties of ferrites depend upon their method of preparation and, because of this, one needs to be extra careful in accurately controlling the conditions of ferrite preparation. The manufacture of polycrystalline ferrites for commercial applications is both an art and a science. A large number of parameters such as the mixing procedure of starting chemicals, firing time and temperature, cooling time, oxygen partial pressure during firing, and many others may be varied to yield different end results. In our sample preparation efforts, a fairly simple version of the standard dry ceramic technique was followed. The starting materials were reagent grade iron oxide, zinc oxide, and manganese carbonate powders. The ferrites were prepared with  $x$  ranging from 0.0 to 1.0 in steps of 0.1 in the formula  $\text{Zn}_x \text{Mn}_{1-x} \text{Fe}_2 \text{O}_4$ .

Using the known molecular weights of starting oxides, appropriate quantities of various oxides were taken in accordance with the solid state reaction



The powders were thoroughly mixed and ground in an agate mortar and pestle for a few hours. The prepared mixture was weighed in a platinum crucible that was placed in a furnace. The temperature of the furnace was gradually raised from room temperature to 1200°C in a period of 2 hours. The samples were fired at this high temperature for about 12 hours in an atmosphere of air. The electric current in the furnace was reduced slowly to bring the temperature down to room temperature in 2 hours.

The resulting product was again ground, weighed, and fired at 1200°C for 12 hours. The ferrite product was then taken out and used as an absorber for the Mössbauer studies. All the samples were prepared twice to determine the reproducibility of the end product.

To ensure that the prepared samples were exactly those intended for study, the following three independent checks were made on the product samples:

1. X-ray powder diffraction
2. Quantitative chemical analysis
3. Saturation magnetization and Curie temperature measurements.

The details of all these methods are given in Reference 6. The results obtained from the above tests strongly indicated that the preparation method of the desired ferrites was satisfactory.

## EXPERIMENTAL PROCEDURE

The basic requirements for the measurement of the Mössbauer effect in  $^{57}\text{Fe}$  systems are: a source containing  $^{57}\text{Co}$ , the sample to be investigated, a scintillation crystal or proportional counter for detecting the gamma rays, a counting system for the gamma rays, and some method of providing a relative velocity to the source with respect to the absorber.

The essential components of a Mössbauer spectrometer are shown as a block diagram in Figure 2. The spectrometer can be divided into three basic subsystems:

1. The velocity drive
2. The gamma-ray detector
3. The data accumulation system.

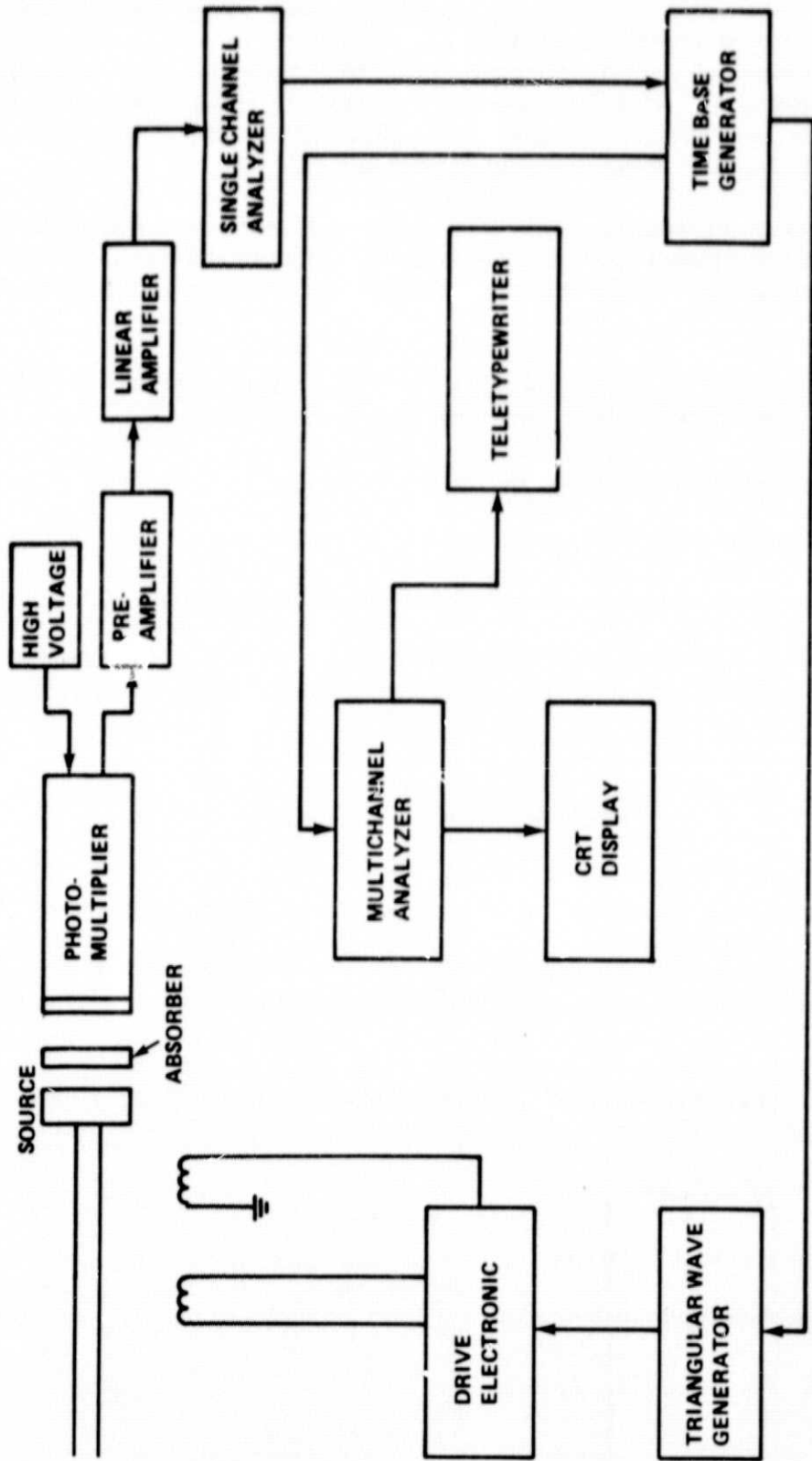


Figure 2. Block diagram of Mössbauer spectrometer.

A constant acceleration electromagnetic drive was used to perform the above studies. More details about the drive and the spectrometer are given in Reference 6. Gamma rays were detected by a 1 cm thick NaI scintillation crystal coupled to a Harshaw photomultiplier tube. A thin beryllium window was used in front of the NaI crystal to cut off 6.3 keV X-rays from the  $^{57}\text{Co}$  source. The drive unit, sample holder, and the detector were arranged so that the gamma rays reaching the detector formed a solid angle of about 1.2 radians at the source. In the present work the drive was operated in the constant acceleration mode. The pulses corresponding to the desired selective 14.4 keV energy were obtained using a single channel analyzer and fed to a 400-multichannel analyzer operated in a time-sequenced storage mode. The number of gamma pulses received in a 1.25 ms interval at different times was recorded in different channels. The output of the multichannel analyzer was recorded on a teletypewriter.

The radioactive source used in the present study was a 5 mCi  $^{57}\text{Co}$  source in a copper matrix. Calibration of the spectrometer was performed using standard iron foil, stainless steel "310" foil, and sodium nitroprusside (SNP) powder.

Before the data were fed to the computer for analysis, a rough visual estimate of the number of Mössbauer lines, their position, and their half-widths was made on the basis of the nature of the spectrum and the known properties of the sample. These parameters were fed to the computer along with counts collected in each channel of the multichannel analyzer. The computer program essentially calculates theoretically the resultant envelope of all the lines assumed to be Lorentzian in shape. The theoretically calculated counts in each channel are compared with the experimentally observed data, and the sum of the weighted square residual is minimized by successive improvements, in small steps, of the initial input parameters. The procedure continues until a convergence criterion is satisfied. The details of the program used are given in Reference 6.

## RESULTS AND DISCUSSION

The observed room temperature Mössbauer spectra of the series  $\text{Zn}_x \text{Mn}_{1-x} \text{Fe}_2\text{O}_4$ , where manganese ions are replaced by zinc ions, with values of  $x$  ranging from 0.0 to 1.0 at intervals of 0.1 are shown in Figures 3 through 13. For calibration purposes, the SNP spectrum was taken with each sample.

Each spectrum of Figures 3 through 5 exhibits a well resolved six-finger Zeeman pattern. The average full width of half maximum (FWHM) of the six lines in each of the spectra is about 0.7 mm/s. The FWHM with stainless steel "310" standard absorber was observed to be 0.32 mm/s. Such a large value of FWHM for the various sextets suggests the possibility of two six-line Zeeman hyperfine patterns overlapping each other. In fact, the computer output of these lines shows a very good fit to two separate six-line Zeeman

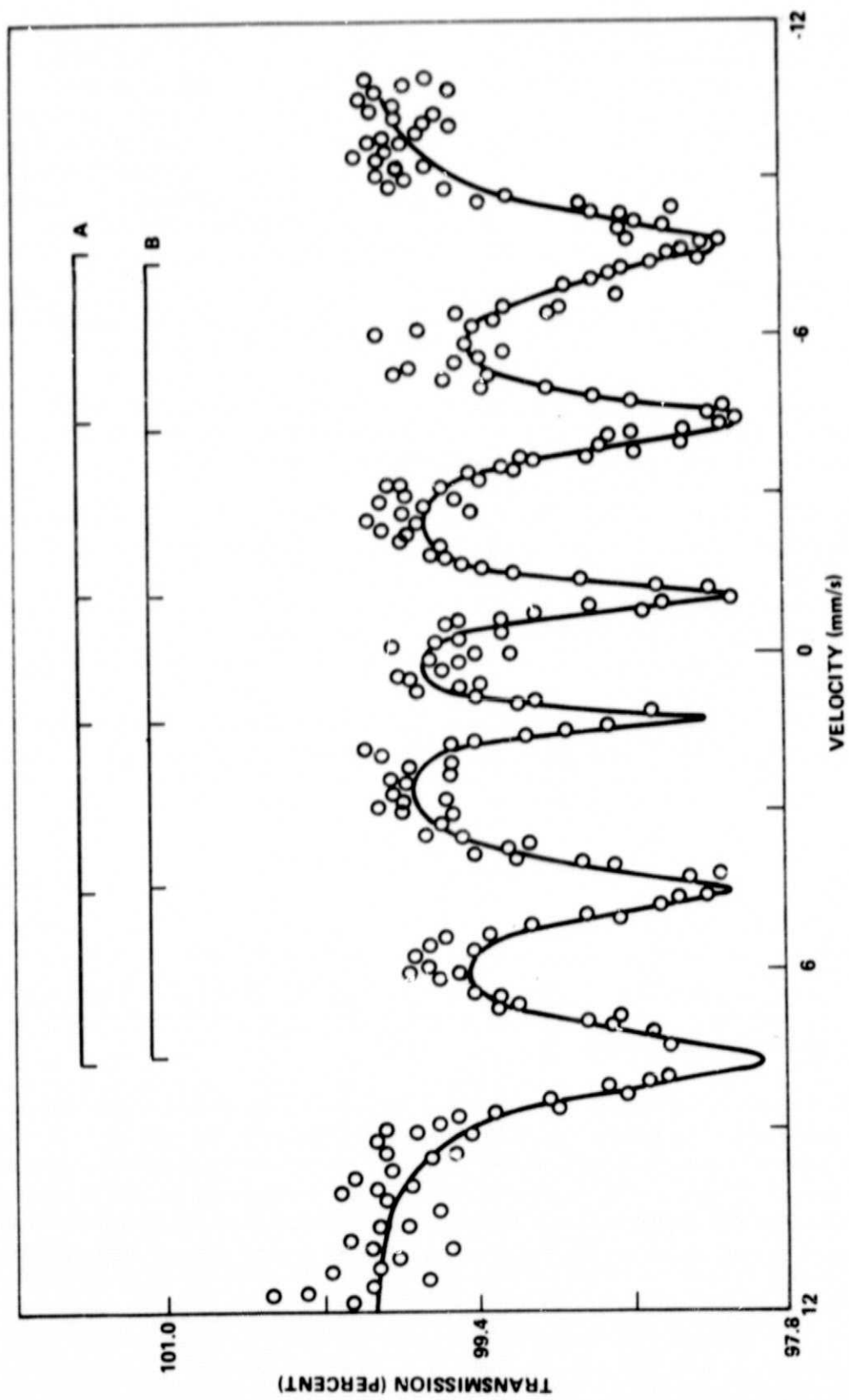


Figure 3. Mössbauer spectrum of  $\text{MnFe}_2\text{O}_4$ .

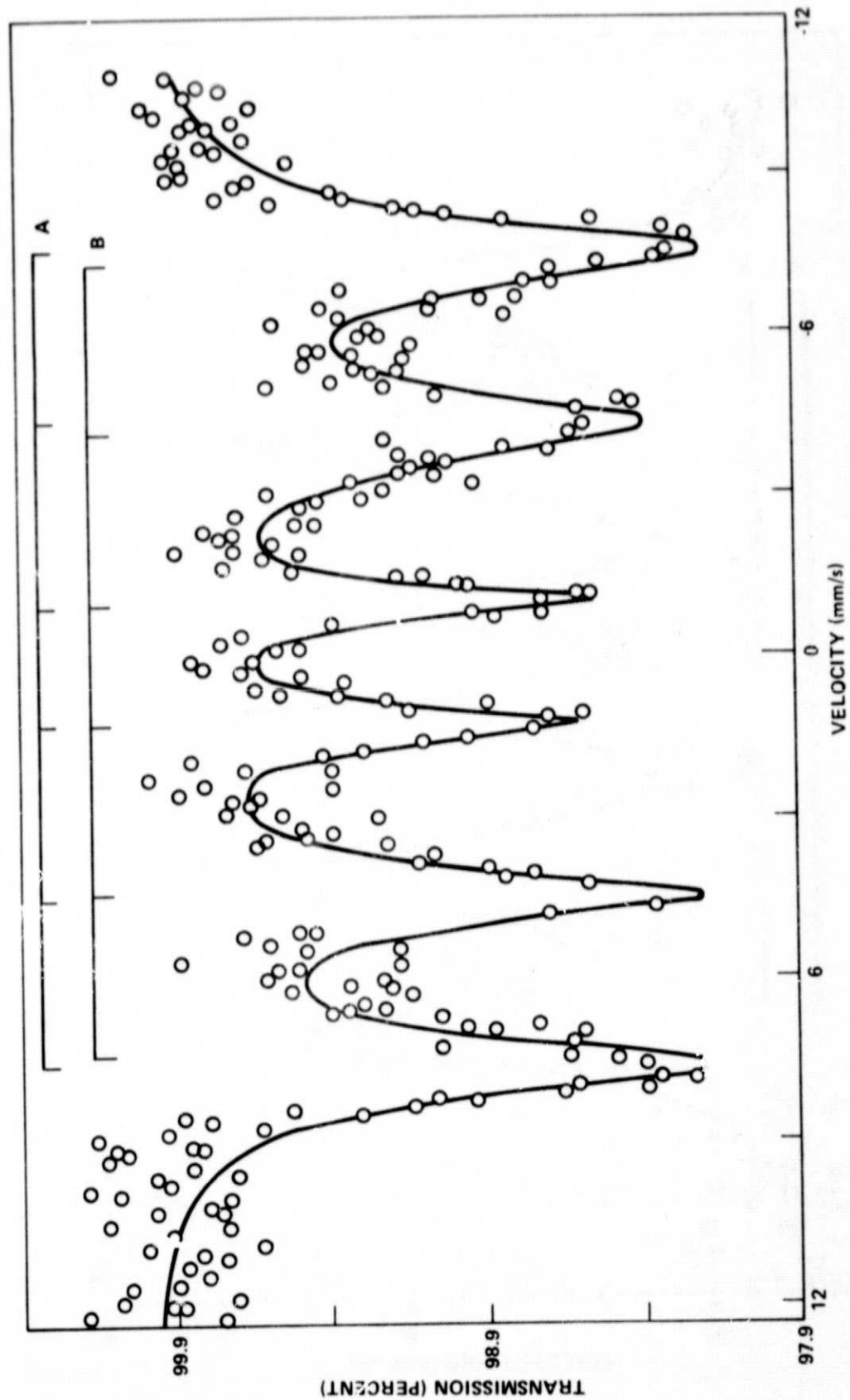


Figure 4. Mössbauer spectrum of  $Zn_{0.1}Mn_{0.9}Fe_2O_4$ .

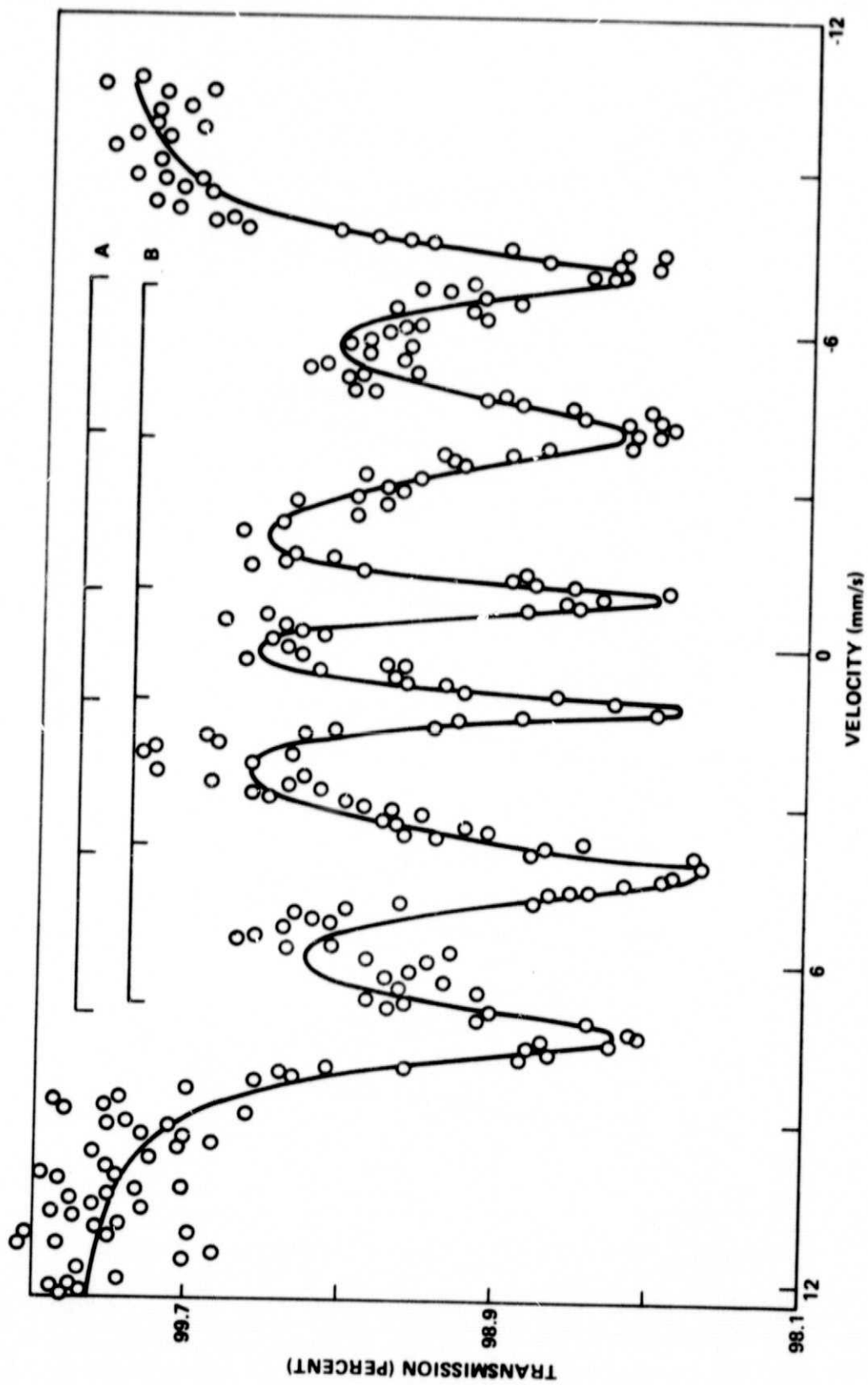


Figure 5. Mössbauer spectrum of  $Zn_{0.2}Mn_{0.8}Fe_2O_4$ .



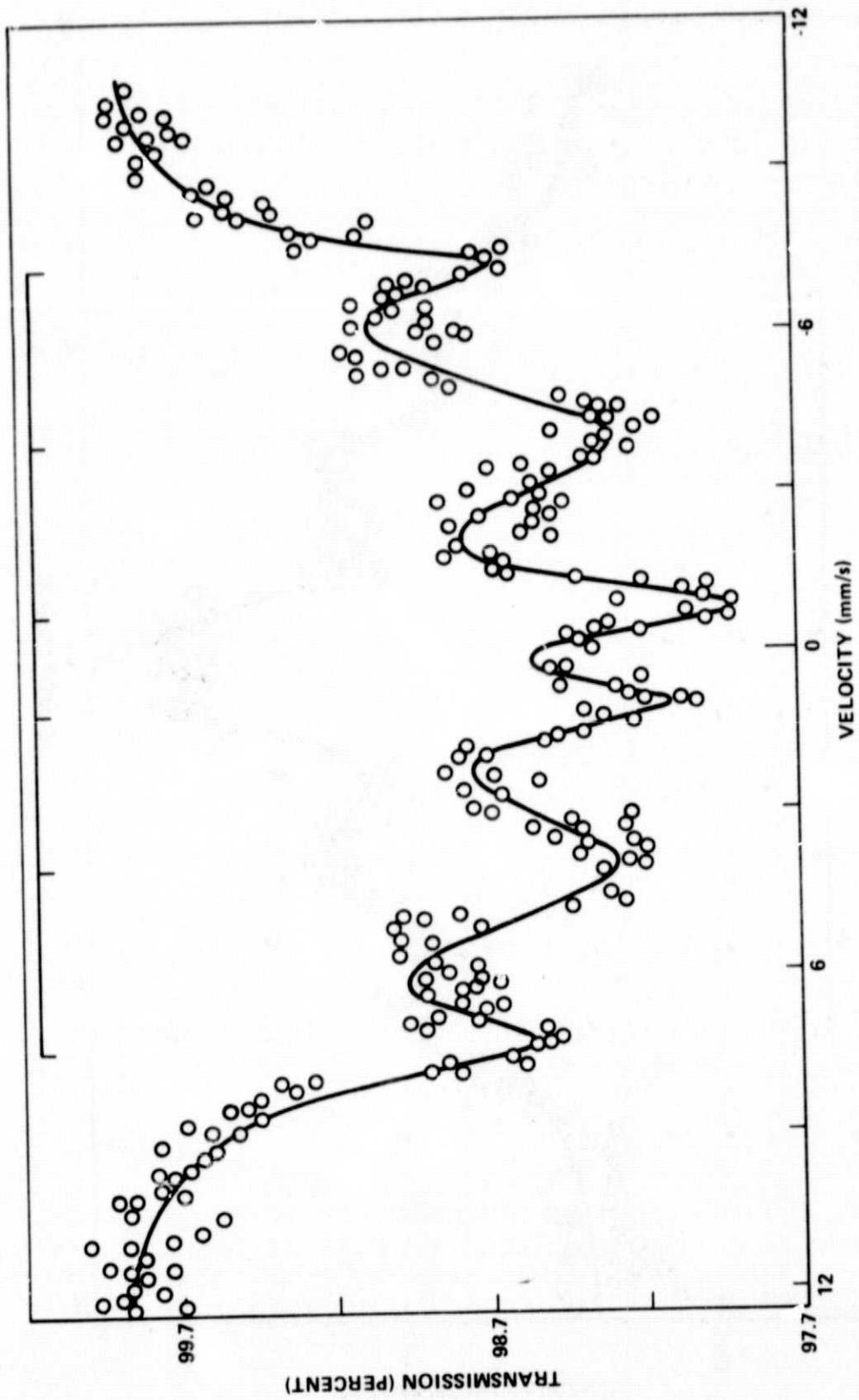


Figure 6. Mössbauer spectrum of  $Zn_{0.3}Mn_{0.7}Fe_2O_4$ .

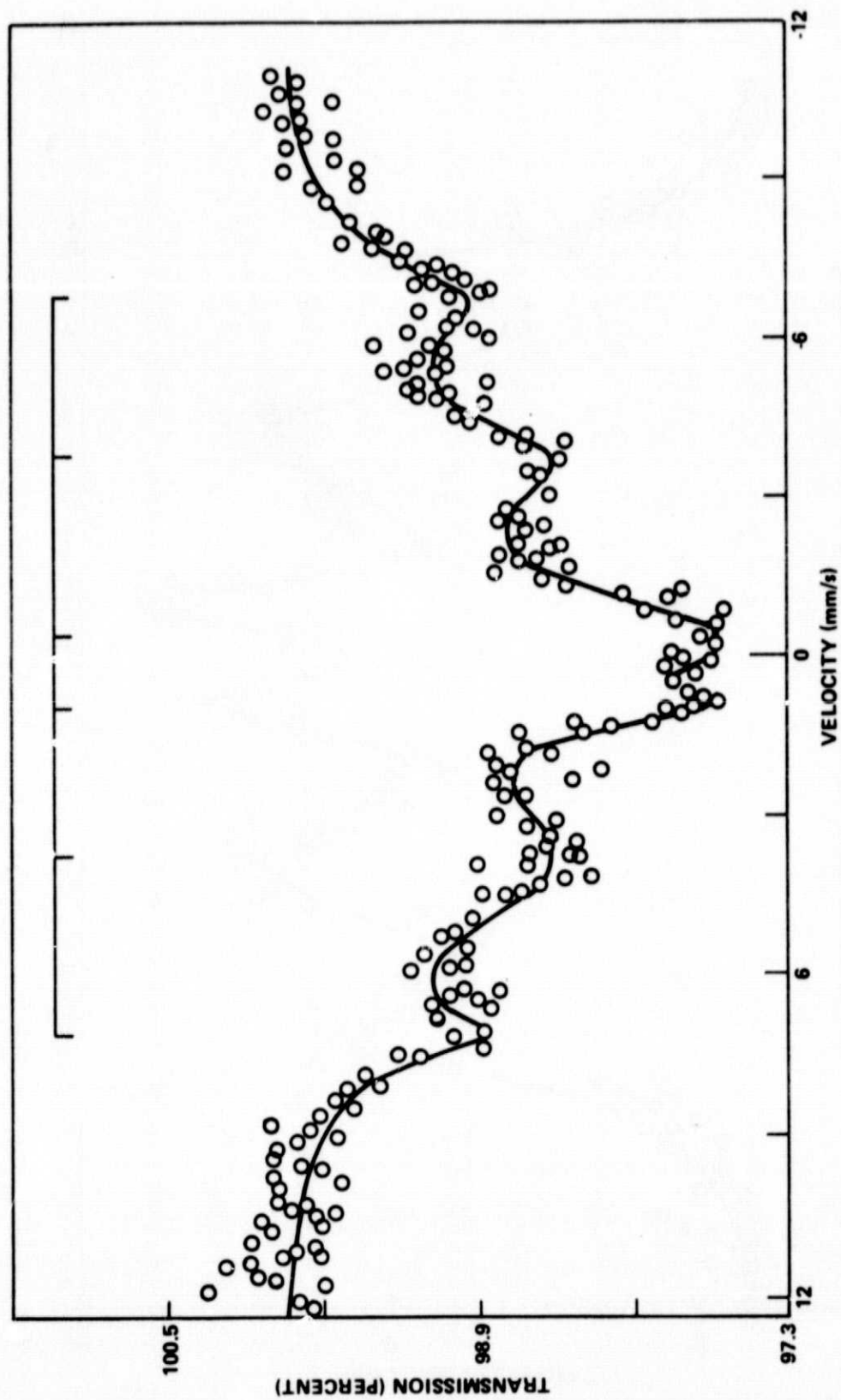


Figure 7. Mössbauer spectrum of  $Zn_{0.4}Mn_{0.6}Fe_2O_4$ .

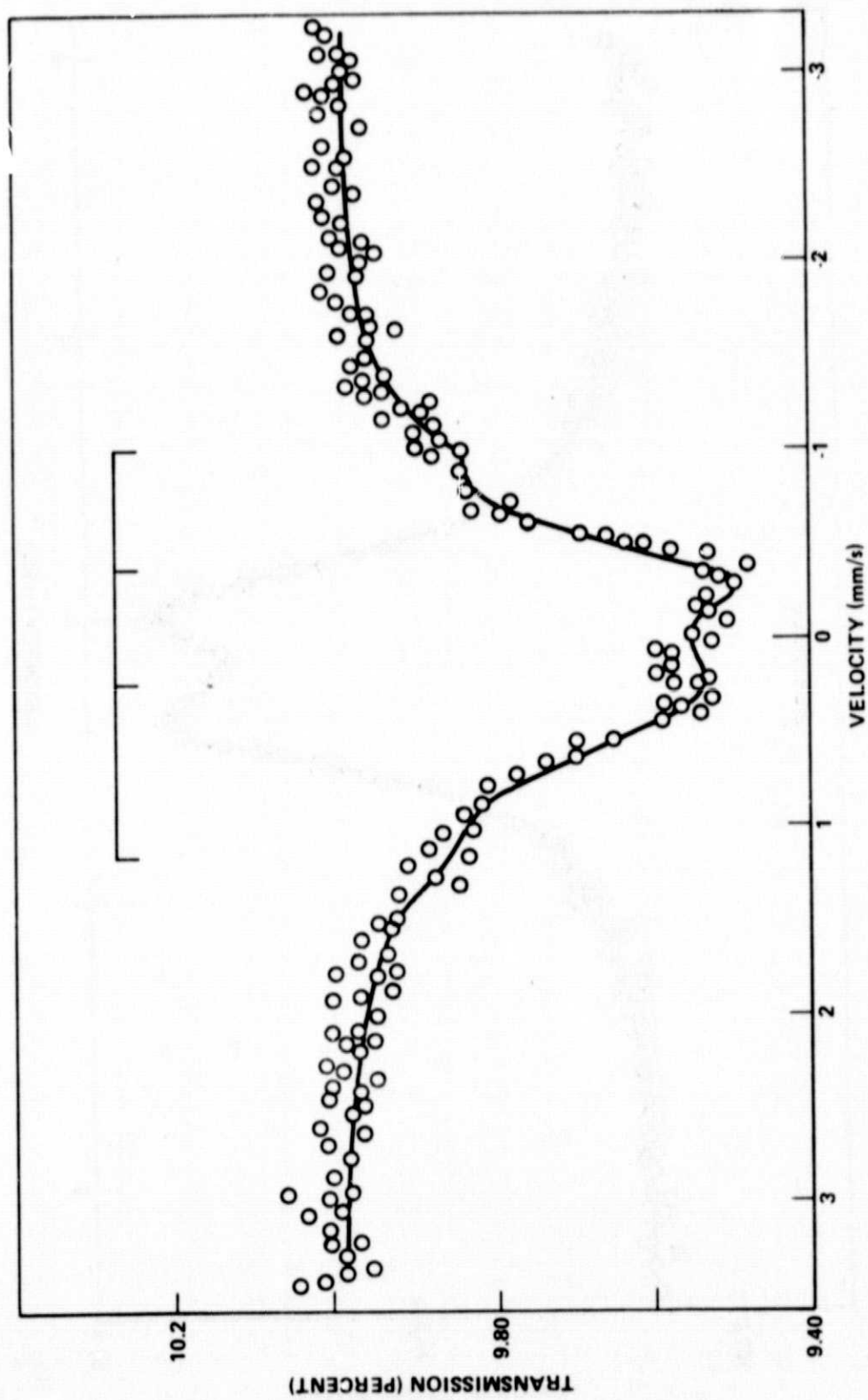


Figure 8. Mössbauer spectrum of  $Zn_{0.5}Mn_{0.5}Fe_2O_4$ .

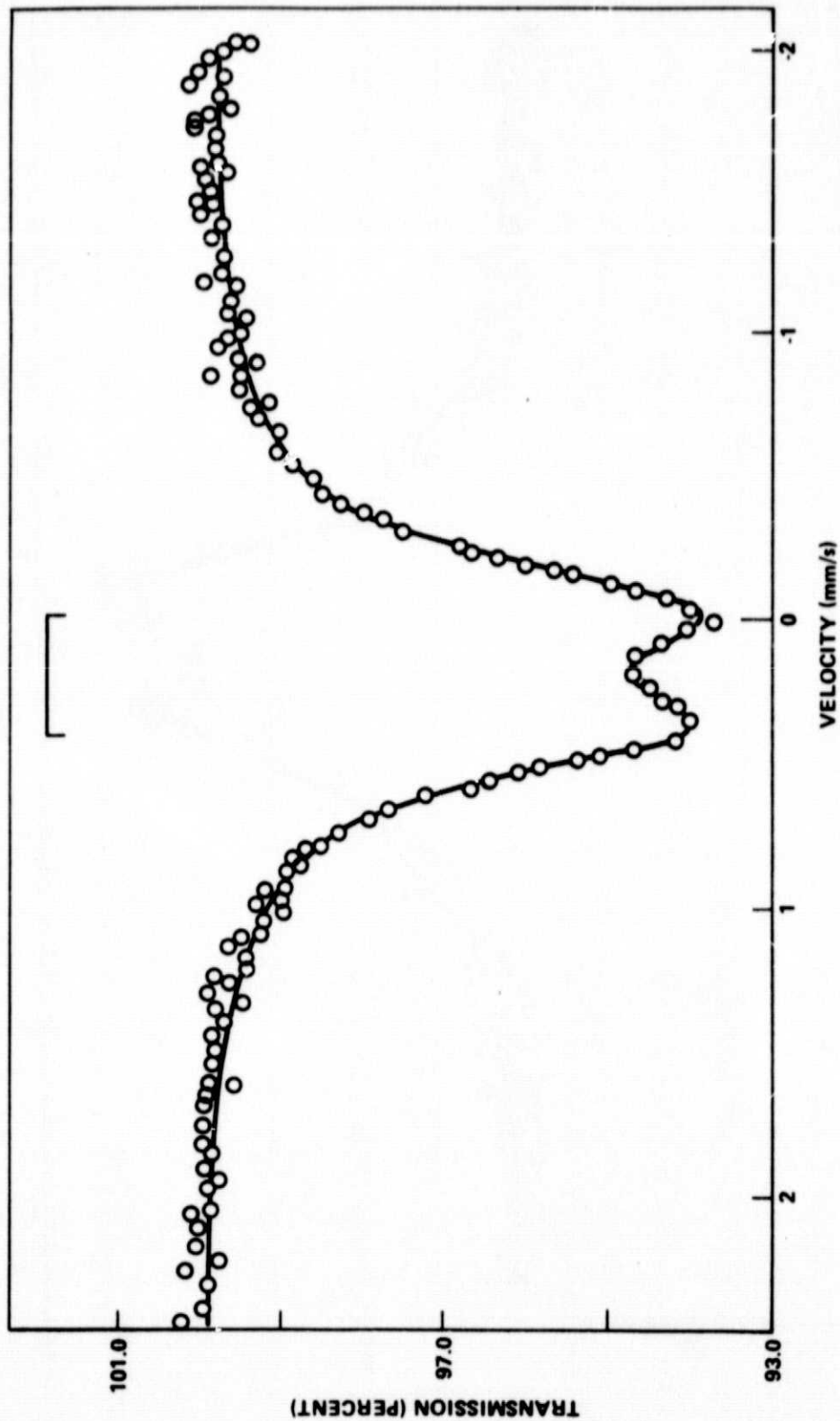


Figure 9. Mössbauer spectrum of  $Zn_{0.6}Mn_{0.4}Fe_2O_4$ .

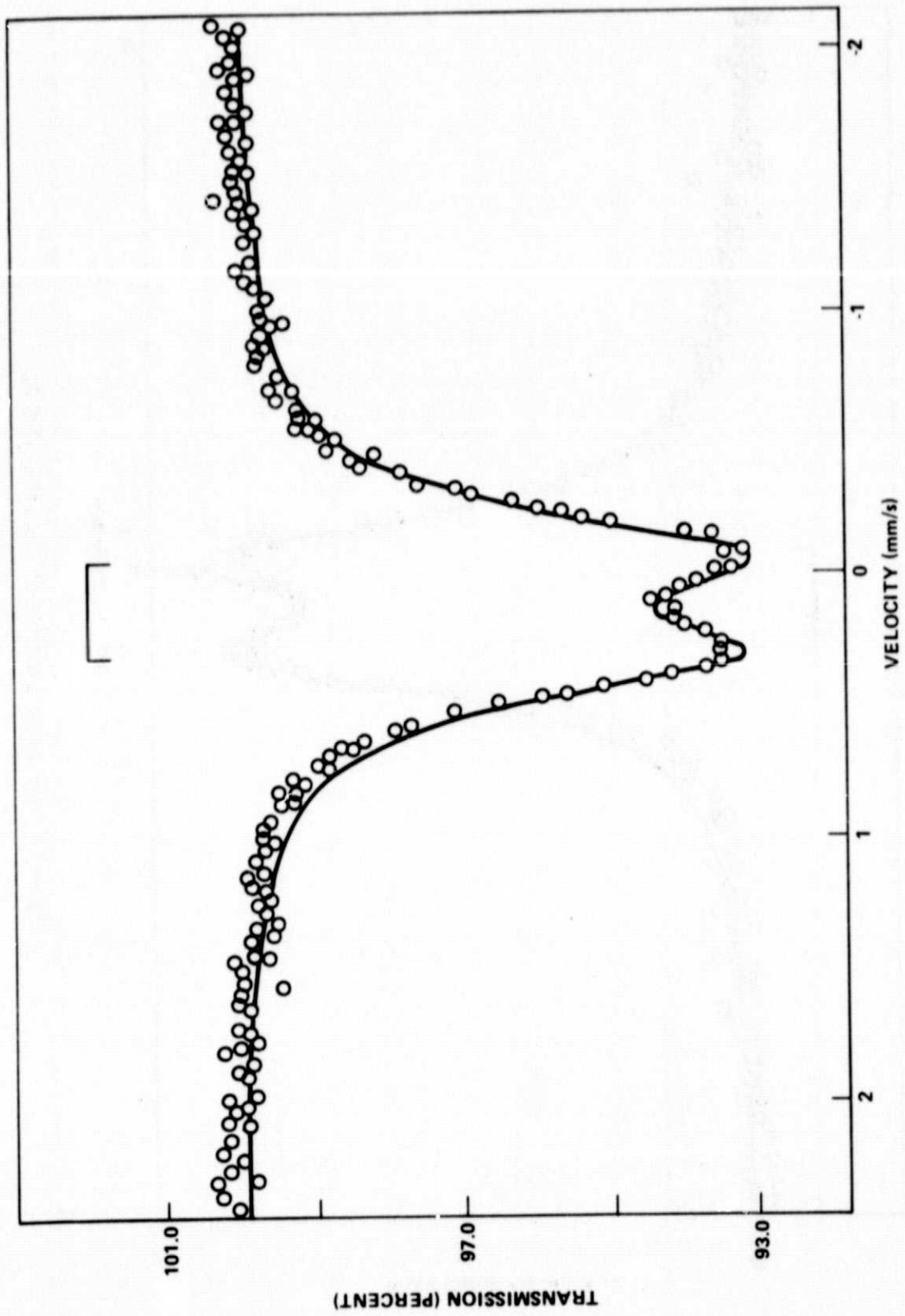


Figure 10. Mössbauer spectrum of  $Zn_{0.7}Mn_{0.3}Fe_2O_4$ .

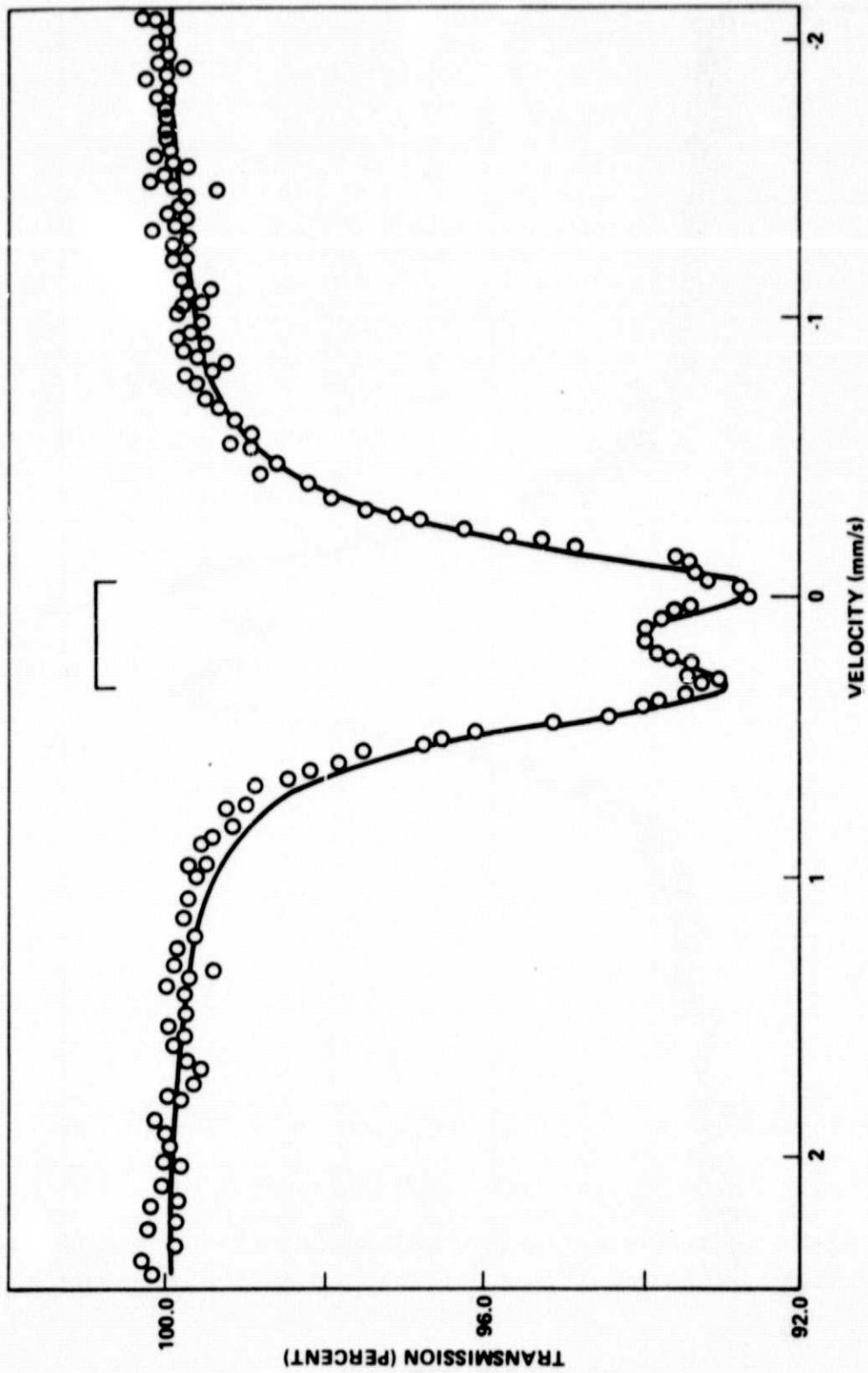


Figure 11. Mössbauer spectrum of  $Zn_{0.8}Mn_{0.2}Fe_2O_4$ .

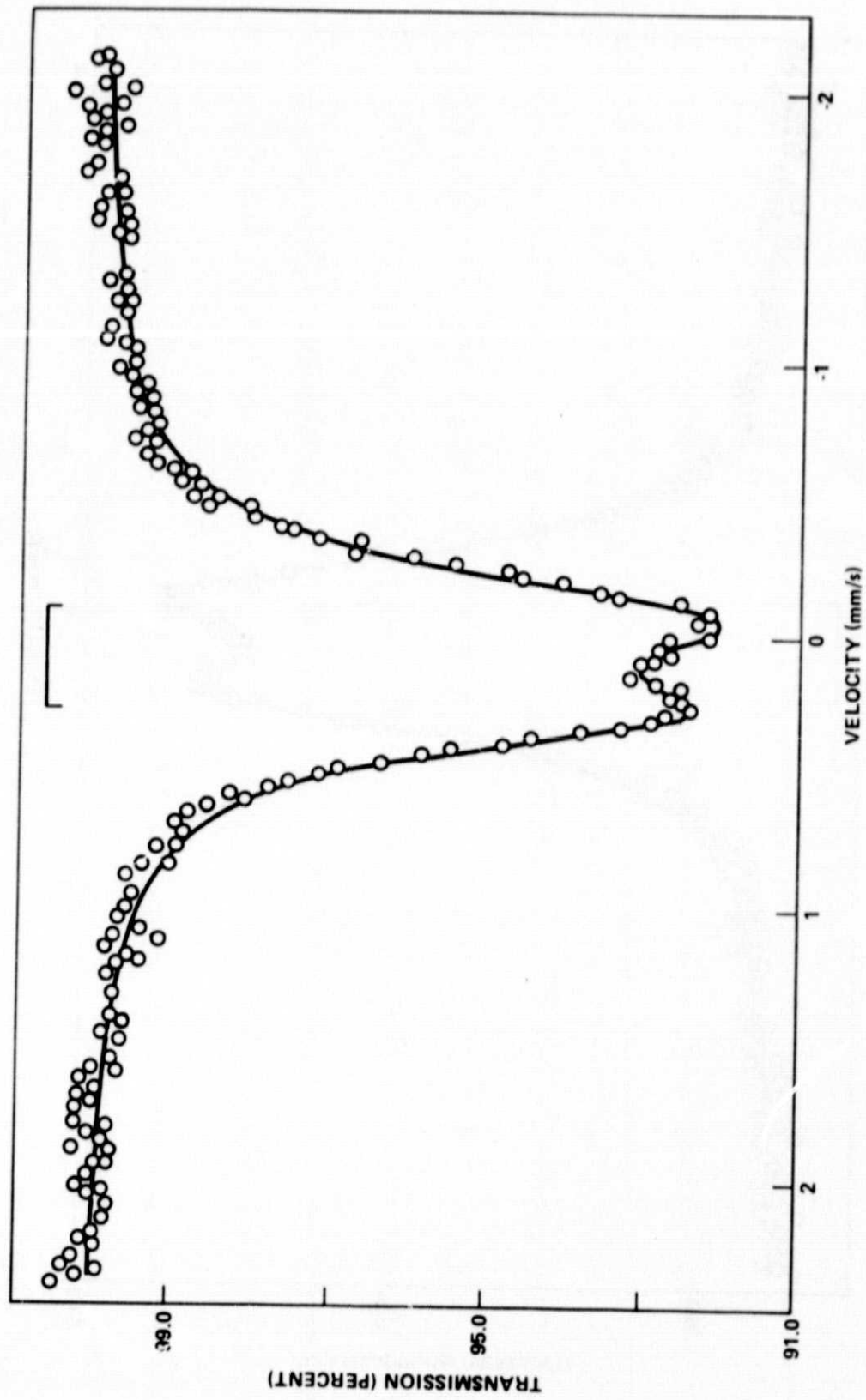


Figure 12. Mössbauer spectrum of  $Zn_{0.9}Mn_{0.1}Fe_2O_4$ .

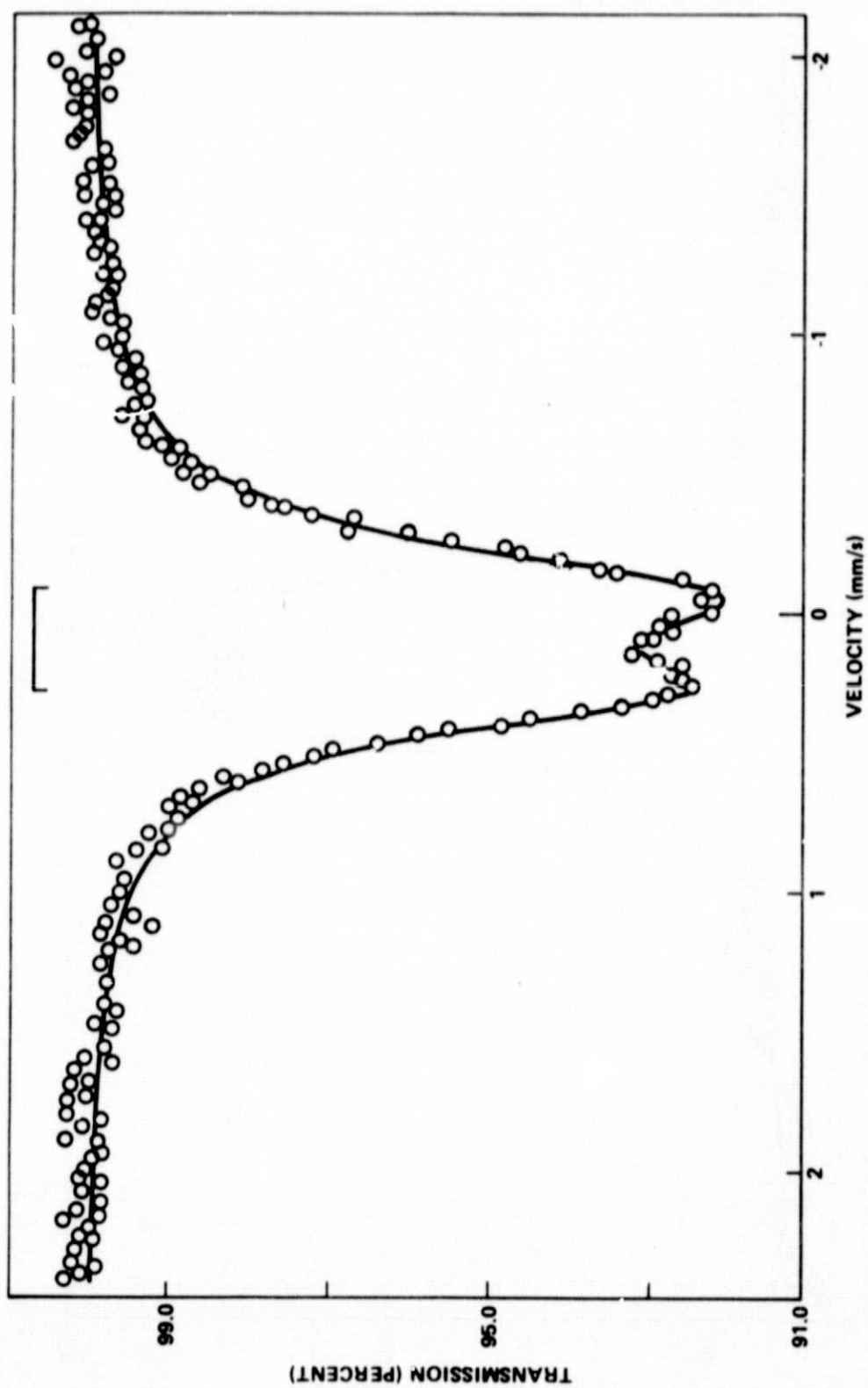


Figure 13. Mössbauer spectrum of  $\text{ZnFe}_2\text{O}_4$ .



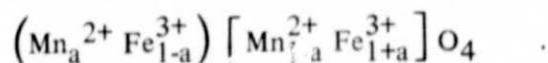
patterns, one due to  $\text{Fe}^{3+}$  ions at the tetrahedral site and the other due to  $\text{Fe}^{3+}$  ions at the octahedral site. Isomer shift and internal magnetic hyperfine field considerations were used to identify the six lines corresponding to the octahedral site and the remaining six lines to the tetrahedral  $\text{Fe}^{3+}$  site. As is explained in Reference 6, the isomer shift for the A-site is always smaller than the isomer shift for the B-site. The internal magnetic hyperfine field, however, is greater at the A-site as compared to that at the B-site. The observed average values of isomer shift of both tetrahedral and octahedral sites lie well within the range of  $\text{Fe}^{3+}$  isomer shift values. There is a definite indication (Table 1) that the isomer shift at the A-site increases while that at the B-site decreases with increasing values of  $x$ .

TABLE 1. ISOMER SHIFT AND MAGNETIC HYPERFINE FIELD FOR SAMPLES HAVING LOW CONCENTRATION OF ZINC

Absorber	Isomer Shift <sup>a</sup> (mm/s)		Magnetic Field (kOe)	
	A-Site	B-Site	A-Site	B-Site
$\text{MnFe}_2\text{O}_4$	$0.0299 \pm 0.18$	$0.121 \pm 0.008$	$475.248 \pm 2.1$	$458.889 \pm 0.9$
$\text{Mn}_{0.9}\text{Zn}_{0.1}\text{Fe}_2\text{O}_4$	$0.0335 \pm 0.018$	$0.114 \pm 0.0115$	$469.539 \pm 2.1$	$448.313 \pm 1.2$
$\text{Mn}_{0.8}\text{Zn}_{0.2}\text{Fe}_2\text{O}_4$	$0.080 \pm 0.018$	$0.109 \pm 0.008$	$449.262 \pm 2.1$	$411.376 \pm 0.9$

a. With respect to Cu source.

As is well established by Verwey and Heilmann [19], only Zn and Cd form the normal ferrites and all other ferrites are known to be inverse ferrites; the degree of inversion varies from ferrite to ferrite. Hastings and Corliss [20] measured the magnetic moment per molecule of manganese ferrite at  $0^\circ\text{K}$  using a neutron diffraction technique. From the results it was concluded that manganese ferrite is not a pure inverse ferrite; instead, it has the following ionic distribution:



This implies that both  $\text{Mn}^{2+}$  ions and  $\text{Fe}^{3+}$  ions exist at the A-site as well as at the B-site. Since zinc has a strong tendency to form a normal ferrite, it will go to the substitutional A-site. There can be two possibilities: zinc replacing  $\text{Mn}^{2+}$  at the A-site or  $\text{Zn}^{2+}$  replacing  $\text{Fe}^{3+}$  at the A-site in which case the  $\text{Fe}^{3+}$  concentration at the B-site increases at the expense of  $\text{Mn}^{2+}$  at the B-site.

In the former possible case the radius of  $Zn^{2+}$  (0.82 Å) is smaller than the radius of  $Mn^{2+}$  (0.91 Å) and the tetrahedron around the zinc ion shrinks, which results in a decrease in the distance between the  $Zn^{2+}$  ion and the four tetrahedrally coordinating oxygen ions. Therefore, there is an increase in the distance of the neighboring  $Fe^{3+}$  ion from the corresponding tetrahedrally coordinating four oxygen ions. The overlapping of  $Fe^{3+}$  at the A-site and the tetrahedrally coordinating oxygen ion orbitals decreases thus increasing the isomer shift. Further, because of the replacement of  $Mn^{2+}$  by zinc, tetrahedron contracts in dimensions which causes a decrease in the distance between the neighboring B-site  $Fe^{3+}$  ions and a few of the six octahedrally coordinating oxygen ions. This, in effect, decreases the isomer shift for the B-site.

In the second possible case, that of  $Zn^{2+}$  replacing iron at A-site, since the  $Zn^{2+}$  radius is larger than the radius of  $Fe^{3+}$  ions (0.67 Å), a decrease in the isomer shift for the A-site should be expected. At the B-site, however, the changes in isomer shift would primarily be a result of the replacement of  $Mn^{2+}$  by  $Fe^{3+}$  at the octahedral site. From the values of ionic radii it follows that the isomer shift for the B-site should increase.

Also, it should be noted from the values of ionic radii that the changes in isomer shift at the A-site because of the first possibility discussed are smaller than the changes observed because of the second possibility. It is, therefore, concluded that the probability of zinc replacing  $Mn^{2+}$  is more than the probability of zinc replacing  $Fe^{3+}$  iron at the A-site. This is a reasonable expectation since the ionic radius of  $Zn^{2+}$  is smaller than that of  $Mn^{2+}$  ions and larger than that of  $Fe^{3+}$  ions. This conclusion is further supported by the observation made in the Mössbauer spectrum taken at higher temperature [6].

Since the bond separation  $Fe^{3+} - O^{2-}$  is large for the octahedral ions as compared to that for the tetrahedral ions, it is obvious that due to the smaller overlapping of the orbitals of  $Fe^{3+}$  ions and oxygen ions, smaller covalency and hence larger isomer shift are expected at the octahedral site. Many experiments have verified this finding [4,8,11,15]. Also, a large decrease in the isomer shift is expected as the coordination number of  $Fe^{3+}$  ions changes from six to four. In general, the isomer shift at the tetrahedral site is smaller than that at the octahedral site. In the presence of an axially symmetric electric field gradient and a strong magnetic field interaction, each of the Zeeman lines is shifted by an amount [21],

$$|\Delta E| = \frac{1}{2} |\Delta E_0| (3 \cos^2 \theta - 1) \quad ,$$

where  $|\Delta E_0|$  is the magnitude of the shift when the magnetic interaction tends to zero, and angle  $\theta$  is the angle between the principal axis of the electric field gradient and the

magnetic field. The presence of chemical disorder in the sample produces a distribution of electric field gradients of varying magnitudes, directions, signs, and asymmetries. In the presence of strong magnetic hyperfine interaction and due to the cubic symmetry of spinel structure, the average of  $(3 \cos^2 \theta - 1)$  is zero. One should not, therefore, see any quadrupole splitting; the Mössbauer lines may be slightly broadened, however. This observation has been made in pure manganese ferrite by many earlier researchers [8,11,14,15]. On the basis of this argument and the fact that the separations between lines 1 and 2 and lines 5 and 6 are the same, the quadrupole splittings present in these samples were assumed to be negligibly small. Internal magnetic hyperfine field and isomer shift as measured from Figures 3 through 5, both at A- and B-sites, are listed in Table 1.

The internal magnetic hyperfine field at the tetrahedral and the octahedral sites arises primarily from the Fermi contact interaction between the nucleus and the spin-polarized S-electrons. The magnetic field at the nucleus is proportional therefore to the atomic magnetic moment and, hence, is proportional to the average magnetization of the A-sublattice. The magnetic field at the Z-site is found larger than the magnetic field at the B-site for  $x$  ranging from 0.0 to 0.2. This is because the manganese ferrite is neither an inverse nor a normal ferrite and because the  $\text{Fe}_A^{3+} - \text{O}^{2-} - \text{Fe}_B^{3+}$  super-exchange A-B bonds as seen by the  $\text{Fe}^{3+}$  ions at the tetrahedral sites are more in number than those seen by the  $\text{Fe}^{3+}$  ions at the octahedral site.

As seen from Table 1, the magnetic field at both the A-site and B-site decreases as the value of  $x$  increases. This increase can be explained on the basis of the change in the number of magnetic bonds. As the content of zinc, which goes and occupies  $\text{Mn}^{2+}$  sites in the A-sublattice, is increased, the number of magnetic bonds ( $\text{Mn}_A^{2+} - \text{O}^{2-} - \text{Fe}_B^{3+}$ ) decreases and, consequently, there is a decrease in the magnetic field at the B-site  $\text{Fe}^{3+}$ . This decrease in the magnetization of the B-sublattice in turn weakens the magnetic influence of the B-sublattice on the A-sublattice. This decreases the B-A interaction as seen by the  $\text{Fe}^{3+}$  ions at the A-site, resulting in a decrease in the magnetization and subsequently in the magnetic field at the  $\text{Fe}_A^{3+}$  nucleus.

It is further obvious from Table 1 that the decrease in the magnetic field at the  $\text{Fe}_B^{3+}$  nucleus is greater than the decrease at the  $\text{Fe}_A^{3+}$  nucleus. This is because the interaction of diamagnetic zinc at the A-site directly influences the magnetic field at the B-site through the A-B interaction, whereas the effect on the  $\text{Fe}_A^{3+}$  nucleus is indirect due to the modified magnetization of the B-sublattice. Thus, the effect on the  $\text{Fe}_A^{3+}$  nucleus can be treated as a second order effect; therefore, one should expect a smaller change in the magnetization of the A-sublattice.

The computer fit of the Mössbauer data presented in Figures 6 through 8 gave six, six, and four Mössbauer lines for  $x = 0.3, 0.4,$  and  $0.5,$  respectively. Attempts to fit two sets of sextets to the observed data corresponding to Figures 6 and 7 revealed that it was

not possible to resolve two sextets corresponding to A- and B-sites. From the appearance of these three spectra, it is quite evident that the relaxation effects are playing an important role in the corresponding samples. In General, the relaxation phenomenon has the following effects on any Mössbauer spectrum [22-26]:

1. Broadening of the lines.
2. A decrease in the separation between lines 3 and 4 and also between lines 1 and 6.
3. An increase in the ratio  $S_{16}/S_{34}$ , where  $S_{16}$  is the distance between the first and the sixth line and  $S_{34}$  is the distance between the third and the fourth line.
4. Merging of lines 1 and 2 and lines 5 and 6; this reduces the outer four lines to two lines.
5. A decrease in the intensity of the outer two lines on either side of middle lines 3 and 4.
6. An increase in the intensity of lines 3 and 4.

The Mössbauer spectra given in Figures 6, 7, and 8 were analyzed on the lines given in Reference 6 to estimate the relaxation effects. The spin flop-flop frequency  $\omega_s$  was estimated and the corresponding spin correlation time  $T_s$  (that is,  $1/\omega_s$ ) was calculated. The values obtained are listed in Table 2.

TABLE 2. VALUES OF SPIN CORRELATION TIME  $T_s$  AND SPIN FLIP-FLOP FREQUENCY  $\omega_s$  FOR A FEW SAMPLES

Absorber	Observed $S_{16}/S_{34}$ (mm/s)	$\omega_s$ (mm/s)	$T_s$ (mm/s)
$MnFe_2O_4$	6.57	0.213	4.694
$Mn_{0.9}Zn_{0.1}Fe_2O_4$	6.65	0.214	4.672
$Mn_{0.8}Zn_{0.2}Fe_2O_4$	6.93	0.299	3.344
$Mn_{0.7}Zn_{0.3}Fe_2O_4$	8.02	0.394	2.538
$Mn_{0.6}Zn_{0.4}Fe_2O_4$	10.40	0.399	2.506

Since the spectrum of Figure 8 does not show six well-resolved clear lines, it was not possible to make similar calculations for the corresponding sample. It is clear from Table 2 that the increase in the relaxation effects as  $x$  increases from 0.0 to 0.2 is small. However, when  $x$  increases from 0.2 to 0.5, the relaxation effects are very marked. It is also concluded from the values of correlation time that the spin flip-flop frequency increases as the concentration of zinc is increased. This can be attributed to the increase in the uniaxial crystalline anisotropy as a result of magnetic annealing in the prepared samples.

Since the internal magnetic hyperfine field is primarily due to the ionic spins, any fluctuations in the latter will result in corresponding fluctuations in the magnetic field at the nucleus. As a magnetic probe, a nucleus will respond, however, to such fluctuations only if they are slow compared to the nuclear Larmor frequency  $\omega_L$ . Thus, if

$$\omega_L \gg \omega_s \quad ,$$

the nucleus does not see the spin relaxation effects and sees only the average value of magnetic field. However, if

$$\omega_L \ll \omega_s \quad ,$$

the relaxation effects become very important and the nucleus does not see any internal magnetic field. As a consequence one observes only a single Mössbauer line. If, however,

$$\omega_L = \omega_s \quad ,$$

one observes an even sextet of the kind shown in Figures 6 and 7.

The correlation time  $T_s$  is related to the anisotropy by the equation [27]

$$T_s = T_0 \exp (KV/kT) \quad ,$$

where  $T_0$  is a constant,  $K$  is the anisotropy per unit volume, and  $V$  is effective volume of the sample. One, in fact, can calculate the exact value of the anisotropy if the average size of the particles of the sample is known.

It is easier to see that when the zinc concentration exceeds a particular limit, one should anticipate the formation of some systematic arrangement of zinc ions in the spinel structure. Any further addition of zinc above this critical value should therefore decrease the anisotropy in this lattice. This would consequently result in a decrease in the correlation time. Such a behavior has been indeed observed by Bozorth et al. [28] in their studies of Zn-doped cobalt ferrite.

From the foregoing discussion it is apparent that the increase in the value of  $x$  weakens the magnetic bonding because of an increase of anisotropy. One should, therefore, expect a decrease in the magnitude of the internal hyperfine magnetic field with an increasing value of  $x$ . A decrease in the internal magnetic field has been indeed observed, as is obvious from Table 1.

For zinc concentration corresponding to  $x$ -values above 0.4, the internal magnetic field becomes so weak compared to the relaxation phenomenon that no hyperfine splitting is observed. It was therefore not possible in the present studies to observe any decrease in the anisotropy and hence any increase in the correlation time.

Since the lines in the Mössbauer spectra of Figures 6 and 7 are not well defined, it is desirable not to place a very high reliability on the conclusions drawn from these two spectra.

The Mössbauer spectra of  $Zn_xMn_{1-x}Fe_2O_4$  with  $x$  ranging from 0.6 to 1.0 (Figs. 9 through 13) each show a quadrupole doublet. One should in fact anticipate three lines except for the case when  $x = 1$ : one due to the tetrahedral  $Fe^{3+}$  ions [9], and the other two as quadrupole doublets due to  $Fe^{3+}$  at the octahedral site. In the present studies however, no line due to  $Fe^{3+}$  at the A-site was observed. This is perhaps because any small amount of iron left at the A-site would give a very faint signal that could be easily overshadowed by the quadrupole doublet due to the octahedral site.

Since  $Fe^{3+}$  ions have half-filled three-dimensional shells, the electric field gradient at the nucleus due to its own electrons is zero. Any electric field gradient would, therefore, arise only because of the lattice contribution. One should, therefore, expect an electric field gradient only at the sites having noncubic point symmetry. Since there is a cubic symmetry around the tetrahedral iron in  $Zn_xMn_{1-x}Fe_2O_4$ , no quadrupole splitting is observed due to the A-site iron. The behavior of the quadrupole splitting because of  $Fe^{3+}$  at the B-site is indicated in Table 3. It is observed that the quadrupole splitting decreases as the value of  $x$  increases from 0.6 to 1.0. This behavior of electric field gradients at B-site iron can be understood as being a result of different ionic sizes of manganese, zinc, and iron ions. As argued in Reference 6, the probability of  $Zn^{2+}$  replacing  $Mn^{2+}$  at the A-site is more than the probability of its replacing the A-site  $Fe^{3+}$  ion. The replacement of A-site  $Mn^{2+}$  by  $Zn^{2+}$  shrinks the tetrahedron around

TABLE 3. ISOMER SHIFT AND QUADRUPOLE SPLITTING IN MIXED Mn-Zn FERRITE WITH A HIGH CONCENTRATION OF ZINC

Absorber	Isomer Shift <sup>a</sup> (mm/s)	Quadrupole Splitting (mm/s)
Mn <sub>0.4</sub> Zn <sub>0.6</sub> Fe <sub>2</sub> O <sub>4</sub>	0.156 ± 0.003	0.416 ± 0.013
Mn <sub>0.3</sub> Zn <sub>0.7</sub> Fe <sub>2</sub> O <sub>4</sub>	0.138 ± 0.003	0.392 ± 0.012
Mn <sub>0.2</sub> Zn <sub>0.8</sub> Fe <sub>2</sub> O <sub>4</sub>	0.142 ± 0.002	0.379 ± 0.011
Mn <sub>0.1</sub> Zn <sub>0.9</sub> Fe <sub>2</sub> O <sub>4</sub>	0.146 ± 0.002	0.351 ± 0.011
ZnFe <sub>2</sub> O <sub>4</sub>	0.199 ± 0.002	0.333 ± 0.011

a. With respect to Cu source.

the Mn<sup>2+</sup> ion keeping the overall cubic symmetry. However, the octahedron around the B-site elongates along the [111] direction and this establishes an electric field gradient at the B-site Fe<sup>3+</sup> ion. As x increases one should therefore expect an increase in the electric field gradient at the octahedral Fe<sup>3+</sup> site. However, when all the manganese at the A-site is replaced by zinc, any further introduction of zinc would replace Fe<sup>3+</sup> at the A-site. Since the radius of the Fe<sup>3+</sup> ion is smaller than that of zinc ion, the tetrahedron now expands and, as a consequence, the octahedron around the B-site iron contracts in the [111] direction. The electric field gradient at the B-site Fe<sup>3+</sup> ion should, therefore, decrease when x increases beyond this particular limit.

In summary, the electric field gradient at the B-site should first increase and then decrease as x increases from 0.0 to 1.0. From the present studies it is evident that the maximum value of the electric field gradient corresponds to the x-value anywhere between 0.3 to 0.5.

### SUMMARY AND CONCLUSIONS

The mixed Mn-Zn ferrite samples, Zn<sub>x</sub>Mn<sub>1-x</sub>Fe<sub>2</sub>O<sub>4</sub> with x ranging from 0.0 to 1.0 in steps of 0.1, were studied at room temperature using the Mössbauer technique.

It was observed that  $Zn^{2+}$  has preference to go and substitute  $Mn^{2+}$  at the A-site. For samples with x-values from 0.0 to 0.2, two internal magnetic hyperfine fields were observed, one at the octahedral and the other at the tetrahedral iron site. The internal magnetic hyperfine field at the tetrahedral iron site is larger than that at the octahedral site. As the value of x was increased, the magnetic field at both the A-site and B-site was observed to decrease in length; the decrease was sharper at the B-site than at the A-site.

The relaxation effects were observed to play an important role as x increased from 0.3 to 0.6. It has been observed that the spin-correlation time decreases with an increasing value of x. This has been attributed to the development of uniaxial anisotropy in the spinel structure as the zinc contents are increased.

Above  $x = 0.6$ , only one quadrupole doublet was observed due to the iron at the octahedral site. The value of the electric field gradient was observed to increase first and then decrease as the value of x was increased from 0.0 to 1.0. The maximum electric field gradient in the present studies was observed to correspond to an x-value somewhere between 0.3 to 0.5.

It is recommended that similar studies should be undertaken at both lower and higher temperatures. This would further reveal the various phenomena taking place in the formation of ferrites. Finally, it can be concluded from the present work that Mössbauer effect data on complex materials, when used in conjunction with other data (X-ray, neutron diffraction, magnetization, etc.), can provide useful insight into the origin of the microscopic properties of magnetic materials.



## REFERENCES

1. Mössbauer, R. L.: *Naturwiss*, vol. 45, 538, 1958.
2. Mössbauer, R. L.: *Z. Physik*, vol. 151, 124, 1958.
3. Mössbauer, R. L.: *Naturforsch*, vol. 14A, 211, 1959.
4. Thanaka, M.; Mizoguchi, T.; and Ailyama, Y.: *J. Phys. Soc. Japan*, vol. 18, 1081, 1963.
5. Belov, V. F.; Deviseva, M. N.; Eludev, I. S.; Markov, E. F.; Stakan, R. A.; Trabanov, V. A.; and Fiz. tverdi.: *Tela*, vol. 6, 3435, 1964.
6. Gupta, R. G.: Ph.D. Thesis, IIT, Delhi.
7. Wieser, E.; Meisel W.; and Kleinstuck K.: *Phys. Stat. Sol.*, vol. 16, 129, 1966.
8. Sawatzky, G. A.; Woude, F. V. D.; and Morrish, A. H.: *Physics Letters*, vol. 25A, 147, 1957.
9. Hundson, A.; and Whitfield, H. J.: *Molecular Physics*, vol. 12, 165, 1967.  
Mizoguchi T.; and Tanka, M. J.: *J. Physic Soc. Japan*, vol. 18, 1301, 1963.
10. Evans, B. J.; Hafnev, S. S.; and Weber, H. P.: *Journal of Chemical Physics*, vol. 55, 5282, 1971.
11. Yagnik, C. M.; and Mathur, H. B.: *Molecular Physics*, vol. 16, 625, 1969.
12. Daniels, J. M.; and Bosencwaig, A.: *Canadian Journal of Physics*, vol. 4, 48, 331, 1970.
13. William, Y. J.: Thesis (A Sutdy of the Mössbauer Effect in the Li-Zn and Co-Zn Ferrites), 1970.
14. Cser, L.; Dezsi, I.; Gladkih, I.; Keszthely, L.; Kulgawezuk, D.; Eissa, N. A.; and Sterk, E.: *Phys. Status Solidi*, vol. 27, 131, 1968.
15. Köing, U.: *Solid State Communication*, vol. 9, 425, 1971.
16. Vleck, J. H. van.: *Phys. Rad.*, vol. 12, 262, 1951.
17. Hagg, G.: *Zs. Fir Physik Chemic*, vol. 29B, 95, 1935.
18. Gorter, E. W.: *Philips Res. Rep*, Vol. 9, 295, 1954; vol. 9, 321, 1954; and vol. 9, 403, 1954.

#### REFERENCES (Concluded)

19. Verwey, E. J. W.; and Heilmann, E. L., Jr.: Chem. Phys., vol. 15, 174, 1947.
20. Hastings, J. M.; and Corliss, L. M.: Phy. Rev., vol. 104, 328, 1956.
21. Matthias, E.; Schneider, W.; and Steffen, R. M.: Phy. Rev., vol. 125, 261, 1962.
22. Woude, F. Vander; and Dekkev, A. J.: Phys. Stat. Sol, vol. 13, 181, 1966.
23. Deszi, I.; and Foder, M.: Phys. Stat. Sol., vol. 15, 247, 1966.
24. Yamamoto, H.; Okada, T.; Watanable, H.; and Fukase, M: J. Phys. Soc. Japan, vol. 24, 275, 1964.
25. Cox, D. E.; Shirane, G.; Flin, P. A.; Ruby, S. L.; and Takei, W. J.: Phys. Rev., vol. 132, 1547, 1963.
26. Jacobi, I. S.; and Beans, C. P.: In Magnetism, vol. 3, chap. 6, 1963.
27. Bozorth, R. M.; Tilden, E. F.; and Williams, A. J.: Phy. Rev., vol. 99, 1788, 1955.
28. Smit, J.; and Wijn, H. P. J.: In Ferrites, 1959.

## APPROVAL

### MÖSSBAUER STUDIES IN ZINC-MANGANESE FERRITES FOR USE IN MEASURING SMALL VELOCITIES AND ACCELERATIONS WITH GREAT PRECISION

The information in this report has been reviewed for security classification. Review of any information concerning Department of Defense or Atomic Energy Commission programs has been made by the MSFC Security Classification Officer. This report, in its entirety, has been determined to be unclassified.

This document has also been reviewed and approved for technical accuracy.

F. B. Moore

F. B. MOORE  
Director, Electronics and Control Laboratory